Golgi Phosphoprotein 3 Confers Radioresistance via Stabilizing EGFR in Lung Adenocarcinoma

Chen, G., Kong, P., Yang, M., Hu, W., Prise, K. M., Yu, K. N., Cui, S., Qin, F., Meng, G., Almahi, W. A., Nie, L., & Han, W. (2021). Golgi Phosphoprotein 3 Confers Radioresistance via Stabilizing EGFR in Lung Adenocarcinoma. *International journal of radiation oncology, biology, physics*. Advance online publication. https://doi.org/10.1016/j.ijrobp.2021.11.023

Published in:
International journal of radiation oncology, biology, physics

Document Version:
Peer reviewed version

Golgi Phosphoprotein 3 Confers Radioresistance via Stabilizing EGFR in Lung Adenocarcinoma

Guodong Chen PhD , Peizhong Kong PhD , Miaomiao Yang MSc , Wanglai Hu PhD , Kevin M. Prise PhD , K.N. Yu PhD , Shujun Cui MSc , Feng Qin MSc , Gang Meng PhD , Waleed Abdelbagi Almahi MSc , Lili Nie MSc , Wei Han PhD

PII: S0360-3016(21)03221-1
DOI: https://doi.org/10.1016/j.ijrobp.2021.11.023
Reference: ROB 27365

To appear in: *International Journal of Radiation Oncology, Biology, Physics*

Received date: 2 December 2020
Revised date: 30 October 2021
Accepted date: 19 November 2021

Please cite this article as: Guodong Chen PhD , Peizhong Kong PhD , Miaomiao Yang MSc , Wanglai Hu PhD , Kevin M. Prise PhD , K.N. Yu PhD , Shujun Cui MSc , Feng Qin MSc , Gang Meng PhD , Waleed Abdelbagi Almahi MSc , Lili Nie MSc , Wei Han PhD , Golgi Phosphoprotein 3 Confers Radioresistance via Stabilizing EGFR in Lung Adenocarcinoma, *International Journal of Radiation Oncology, Biology, Physics* (2021), doi: https://doi.org/10.1016/j.ijrobp.2021.11.023

Golgi Phosphoprotein 3 Confers Radioresistance *via* Stabilizing EGFR in Lung Adenocarcinoma

GOLPH3 Confers Radioresistance in LUAD

Guodong Chen, PhD,[1,2*] Peizhong Kong, PhD,[1,2*] Miaomiao Yang, MSc,[1,3,4] Wanglai Hu, PhD,[5] Kevin M. Prise, PhD,[6] K.N. Yu, PhD,[7,8] Shujun Cui, MSc,[1,3] Feng Qin, MSc,[1,3] Gang Meng, PhD,[4,9] Waleed Abdelbagi Almahi, MSc,[1,3] Lili Nie, MSc,[1,2] Wei Han, PhD,[1,2,10#]

[1] Anhui Province Key Laboratory of Medical Physics and Technology, Institute of Health and Medical Technology, Hefei Institutes of Physical Science, Chinese Academy of Sciences, Hefei, 230031, P. R. China

[2] Hefei Cancer Hospital, Chinese Academy of Sciences, Hefei, 230031, P. R. China

[3] University of Science and Technology of China, Hefei, 230026, P. R. China

[4] Clinical Pathology Center, The Fourth Affiliated Hospital of Anhui Medical University, Hefei, 230012, P. R. China

[5] School of Basic Medical Science, Anhui Medical University, Hefei, Anhui, 230027, P. R. China

[6] Centre for Cancer Research & Cell Biology, Queen's University Belfast, Belfast, BT7 1NN, United Kingdom

[7] Department of Physics, City University of Hong Kong, Tat Chee Avenue, Kowloon Tong, 999077, Hong Kong

[8] State Key Laboratory in Marine Pollution, City University of Hong Kong, Tat Chee Avenue, Kowloon Tong, 999077, Hong Kong

[9] Department of Pathology, Anhui Medical University, Hefei, 230032, P. R. China

[10] Collaborative Innovation Center of Radiation Medicine of Jiangsu Higher Education Institutions and School for Radiological and Interdisciplinary Sciences (RAD-X), Soochow University, Suzhou, 215006, P. R. China.

*: These authors contributed equally to this work.

[#]: Corresponding author

[Corresponding Author Name & Email Address]

Wei Han, Email address: hanw@hfcas.ac.cn

[Author Responsible for Statistical Analysis Name & Email Address]

Peizhong Kong, Email address: gckongpz@163.com

[Conflict of Interest Statement for All Authors]

Conflict of Interest: None

[Funding Statement]

This research was supported by the Chinese National Natural Science Foundation (grant nos. 81703168, U1632145 and 81227902), the Natural Science Fund of Anhui Province (608085QH181), Natural Science Foundation of the Higher Education Institutions of Anhui Province (KJ2017A826), CASHIPS Director's Fund (grant no.YZJJ2018QN19) and project funded by the Priority Academic Program Development of Jiangsu Higher Education Institutions (PAPD) and Jiangsu Provincial Key Laboratory of Radiation Medicine and Protection. This research was also supported by the research grant IRF/0024 from the State Key Laboratory in Marine Pollution, City University of Hong Kong.

[Data Availability Statement for this Work]

Research data are stored in an institutional repository and will be shared upon request to the corresponding author.

[Acknowledgements]

None

Abstract

Purpose: Radioresistance is a major cause of treatment failure in tumor radiotherapy and the underlying mechanisms of radioresistance are still elusive. Golgi phosphoprotein 3 (GOLPH3) has been reported to associate tightly with cancer progression and chemoresistance. Herein, we explored whether GOLPH3 mediated radioresistance of lung adenocarcinoma (LUAD) and whether targeted suppression of GOLPH3 sensitized LUAD to radiotherapy.

Methods and Materials: The aberrant expression of GOLPH3 was evaluated by immunohistochemistry in LUAD clinical samples. To evaluate the association between GOLPH3 and radioresistance, colony formation and apoptosis were assessed

in control and GOLPH3 knockdown cells. γ-H2AX foci/level determination and micronucleus test were used to analyze DNA damage production and repair. The rescue of GOLPH3 knockdown was then performed by exogenous expression of siRNA-resistant mutant GOLPH3 to confirm the role of GOLPH3 in DNA damage repair. Mechanistically, the effect of GOLPH3 on regulating stability and nuclear accumulation of epidermal growth factor receptor (EGFR) and the activation of DNA-PK were investigated by qRT-PCR, western blot, immunofluorescence and co-immunoprecipitation. The role of GOLPH3 *in vivo* in radioresistance was determined in a xenograft model.

Results: In tumor tissues of 33 patients with LUAD, the expression of GOLPH3 showed significantly increases compared with those in matched normal tissues. Knocking down GOLPH3 reduced the clonogenic capacity, impaired DSB repair and enhanced apoptosis after irradiation. In contrast, reversal of GOLPH3 depletion rescued the impaired repair of radiation-induced DSBs. Mechanistically, loss of GOLPH3 accelerated the degradation of EGFR in lysosome, causing the reduction in EGFR levels, thereby weakening nuclear accumulation of EGFR and attenuating the activation of DNA-PK. Furthermore, adenovirus-mediated GOLPH3 knockdown could enhance the ionizing-radiation response in LUAD xenograft model.

Conclusions: GOLPH3 conferred resistance of LUAD to ionizing-radiation *via* stabilizing EGFR and targeted suppression of GOLPH3 might be considered as a potential therapeutic strategy for sensitizing LUAD to radiotherapy.

Keywords: Radioresistance, Golgi Phosphoprotein 3, EGFR, DNA-PK, DSB repair

Introduction

Lung cancer, a leading cause of cancer mortality in the world, has been estimated to have 1.8 million deaths worldwide in 2020.[1] Based on histology, lung cancer can be classified either as small cell lung cancer (SCLC) or non-small cell lung cancer (NSCLC), and the latter accounts for approximately 80% of all lung cancers. Radiotherapy is increasingly used due to its advandages for lung cancer patients, especially inoperable cases, besides surgery and chemotherapy. Optimization of radiotherapy is necessary for treating NSCLC due to a relatively higher radioresistance, especially of lung adenocarcinoma which is the most frequently encountered among NSCLC cases.[2]

Tumor cell radioresistance, one of the most important determinants in therapy planning and prognosis, is tightly associated with its genetic background.[3] Previous studies have revealed various radiorsistance associated genes such as P53,[4] STAT3,[5] and EGFR.[6,7] Highly expressed EGFR were present in most cases of NSCLC,[8] and associated with chemotherapy resistance.[9] Furthermore, it is known that abnormal activity or overexpression of EGFR usually cause radioresistance in NSCLC,[10] and targeting EGFR to increasing ionizing radiation (IR) sensitivity has been preclinically tested.[11] Nuclear EGFR has been found to play a key role in preventing tumor cell death *via* activating DNA-PKcs dependent DNA double-strand break (DSB) repair following treatment with cisplatin or IR.[12]

Golgi phosphoprotein 3 (GOLPH3) protein, also known as GPP34, GMx33, MIDAS or Vps74p, is a component of trans-Golgi network (TGN) which functions as

a late secretory sorting station. Recently, GOLPH3 has also been identified as a new oncoprotein, which is commonly overexpressed in human cancers including breast cancer,[13] hepatocellular carcinoma,[14] prostate cancer,[15] and NSCLC.[16,17] In addiation, clinical data also demonstrate that GOLPH3 functions as an independent prognostic marker for early-stage NSCLC patients after surgery,[16] and overexpression of GOLPH3 is associated with poor survival in NSCLC patients.[17] Oncogenes frequently play an important role in determining drug resistance, and there is no exception for GOLPH3. It is confirmed that GOLPH3 overexpression and decreased level of miR34a promote enrichment of cancer stem cells and chemoresistance.[18] Indeed, depletion of GOLPH3 causes a significant increase in cellular apoptosis in response to doxorubicin and camptothecin depending on the Golgi dispersal regulated by the DNA-PK/GOLPH3/MYO18A signaling pathway.[19] Due to modulation of mTOR signalling by regulating receptor recycling of the upstream key molecules, GOLPH3 confers increased sensitivity to rapamycin in cancer.[20] Therefore the expression level, as well as gene copy-number status of GOLPH3, may be useful predictors of cellular sensitivity to mTOR inhibitors. Although some evidence suggested that GOLPH3 may be a predictive marker of clinical response to DNA-damaging chemotherapy, whether GOLPH3 plays an important role in resistance of NSCLC to IR which also causes DNA damage, is still unknown.

In the present study, overexpression of GOLPH3 was observed in collected LUAD clinical tissue samples, and knocking down GOLPH3 sensitized LUAD cells to X-ray irradiaition *via* impairing DSBs repair. Furthermore, a novel signaling pathway

GOLPH3/EGFR/DNA-PK in which GOLPH3 stablized EGFR, enhanced the nuclear accumulation of EGFR and activated DNA-PK after IR, was found to be involved in radioresistance. *In vivo* study also confirmed that GOLPH3-KD enhanced the growth delay of LUAD xenograft after IR exposure. These results suggested that the expression level of GOLPH3 in LUAD was tightly correlated with the radioresistance, and targeting GOLPH3 might be considered as a therapeutic strategy for sensitizing LUAD cells to radiotherapy.

Methods and Materials

Cell culture

The LUAD cell lines A549 and NCI-H1299 were purchased from the Cell Bank of Type Culture Collection of Chinese Academy of Sciences (Shanghai, China). The NCI-H522, NCI-H1975, NCI-H322 and NCI-H1793 cell lines were purchased from the American Type Culture Collection (ATCC, Manassas, VA, USA). The PC9 line was purchased from Sigma-Aldrich (St. Louis, MO, USA). The A549, NCI-H1299, NCI-H522, NCI-H1975, NCI-H322 as well as PC9 cell lines were cultured in RPMI 1640 medium (HyClone; GE Healthcare Life Sciences, Logan, UT, USA), supplemented with 10% fetal bovine serum (FBS, HyClone) , 100 μg/mL streptomycin (Gibco, Carlsbad, CA, USA) and 100 U/mL penicillin (Gibco). NCI-H1793 was cultured in DMEM:F12 medium (HyClone), supplemented with 0.005 mg/mL insulin (Sigma-Aldrich), 0.1 mg/mL transferrin (Sigma-Aldrich), 30 nM sodium selenite (Sigma-Aldrich), 10 nM hydrocortisone (Sigma-Aldrich), 10 nM beta-estradiol (Sigma-Aldrich), 2 mM L-glutamin (Sigma-Aldrich) and 5% FBS

(HyClone). All cell lines were maintained at 37°C in a humidified 5% CO_2 incubator. And all cell lines were free of mycoplasma.

Irradiation

The cells were irradiated with a series of doses (0-6 Gy) by using an XHA600D X-ray irradiator (SHINVA, Zibo, Shandong, China) at a dose rate of 0.189 Gy/min. The culture medium was replaced with fresh medium before irradiation.

Retroviral and adenovirus infection

The plasmids, phU6-GOLPH3-RNAi-puro and phU6-EGFR-RNAi-puro, were generated by subcloning human GOLPH3- and EGFR-targeting short hairpin RNA (shRNA) oligonucleotides sequences into the lentiviral vector GV248 or GV112 (Shanghai GeneChem Co., Ltd., Shanghai, China). The shRNA target sequences of GOLPH3 were: RNAi#1, GCATGTTAAGGAAACTCAGCC; RNAi#2, GCAGCGCCTCATCAAGAAAGT. The shRNA target sequences of EGFR were: RNAi#1, CACAAAGCAGTGAATTTAT; RNAi#2, CAAGCCAAATGGCATCTTT. Lentiviruses were prepared by co-transfecting HEK293T cells with a phU6-RNAi-puro vector, containing shRNAs against GOLPH3 or EGFR, and the packaging plasmids psPAX2 and pMD2.G, as described previously.[21] A549 and H1299 cells were infected with the lentiviruses and the stable cell lines expressing GOLPH3 or EGFR shRNA were selected for 10 days with puromycin (2 μg/mL) from 48 h after infection.

For the rescue experiments, the wild-type GOLPH3 expression plasmid was mutagenized by PCR to generate an RNAi-resistant isoform ($GOLPH3^{Res}$) which

contained five silent mutations (aCAaCGgCTaATCAA- GAAgGT) introduced into the region targeted by GOLPH3-RNAi#2. The isoform was subcoloned into the shuttle vector pHBAd-MCMV-IRES-EGFP (fused with a N-terminal 3×FLAGs tag) and the adenovirus with a titer of 5×10^{10} PFU/mL was prepared by Hanbio Co., Ltd. (Shanghai, China). After adenovirus infection, western blot and immune-fluorescence assay were administrated to detect varied protein expressions and the level of DSBs induced by IR.

Colony formation assay

Cells of A549 (300 cells) and H1299 (200 cells) were seeded in 60 mm dishes after irradiation and then incubated for 8 days to form colonies. Survival curves were constructed by using the Origin 8.0 software. The survival curve parameters, D0 and Dq, were calculated by fitting the data with the single-hit multi-target model.[22]

Flow cytometric analysis

Cells were harvested at 72 h after irradiation and apoptotic cells were stained with annexin V-APC/PI kit according to the manufacturer's instructions (BD Biosciences, San Jose, CA, USA) and then analyzed with a BD Accuri C6 analyzer (BD Biosciences).

Micronucleus test

The frequency of micronucleus formation was determined according to the *in vitro* micronucleus technique.[23] Cells were trypsinized and 5×10^{4} cells were seeded in 35 mm dishes. Cytochalasin B (Sigma-Aldrich) was added into the culture medium with

a final concentration of 1 μg/mL at 2 h after irradiation. After two doubling time incubation, the cells were fixed with 4% paraformaldehyde (Sigma-Aldrich) for 30 min, stained with 0.1% acridine orange (Sigma-Aldrich) for 3 min, washed with PBS and then viewed under a DMI4000B microscope (Leica, Wetzlar, Germany). The number of micronucleated cells in at least 1000 binucleate (BN) cells was scored and the frequencies of MN per 1000 BN cells were calculated.

Immunofluorescence

Cells were fixed with 4% paraformaldehyde for 30 min and permeabilised with TNBS solution (PBS supplemented with 0.5% Triton X-100 and 1% FBS) for 1 h. The cells were then incubated for 2 h with specific primary antibodies for different proteins as follows: anti-γ-H2AX (phospho S139) antibody (1:200; Abcam, Cambridge, MA, USA) or anti-EGFR antibody (1:200; Abcam) at 37°C. After rinsing in TNBS three times, the cells were incubated for 1 h with Goat Anti-Rabbit IgG H&L (TRITC) (1:1000; Abcam) at 37°C. DAPI (5 mg/mL; Sigma-Aldrich) was used to stain the nuclei. The cells were visualized with a DMI4000B microscope (Leica). At least 200 cells were counted for each group to calculate the number of γ-H2AX foci per cell. To further detect the subcellular localization of EGFR, the images of EGFR staining were captured using a LSM710 confocal laser scanning microscope (Zeiss, Oberkochen, Germany).

Immunohistochemistry

Tumor specimens of human lung adenocarcinoma were collected from patients registered at the XXXX during 2012-2017. The age of patients ranged from 41 to 78

years with the median age as 60 years. The use of human tissues was approved by the Ethics Committee of the hospital. The tumor specimens or excised xenografts were fixed with 10% buffered formalin and embedded in paraffin. Tumor sections were cut into sections (3 μm), and then slices were deparaffinized and rehydrated. These prepared slides were incubated at 4°C overnight with primary antibodies as follows: anti-GOLPH3 (1:100; Abcam), anti-EGFR (1:100; Abcam) or anti-Ki67 (1:1000; Protein Tech Group, Wuhan, China), followed by a 30 min incubation in HRP-conjugated goat anti-rabbit IgG H&L (1:200; Abcam). After washing, slices were incubated with streptavidin peroxidase and visualized using DAB substrate (Beyotime Biotechnology, Shanghai, China). The expression of GOLPH3 and EGFR were quantified by using ImagePro Plus (Media Cybernetics, USA). The mean optical density (MOD) of the selected area [integrated optical density (IOD)/unit area] represented the expression level of the indicated protein.

Subcellular fractionation, western blot and co-immunoprecipitation

Cytoplasmic and nuclear extracts were acquired using the NE-PER® nuclear and cytoplasmic extraction kit (Pierce, Rockford, IL, USA). Whole-cell protein was extracted with RIPA lysis buffer (Beyotime Biotechnology) and the protein concentration was determined with a BCA protein assay kit (Beyotime Biotechnology). Briefly, proteins were separated by 6-15% sodium dodecyl sulfate-polyacrylamide gel electrophoresis (SDS-PAGE) and transferred to polyvinylidene fluoride membranes (Merck Millipore, Darmstadt, Germany). Membranes were blocked in 5% skim milk (BD/Difco, Sparks, MD, USA) for 1 h,

and then incubated with different primary antibodies at 4°C overnight. The primary antibodies utilized were: anti-GOLPH3 (1:1000; Abcam), anti-EGFR (1:1000; Protein Tech Group), anti-gamma H2AX (phospho S139) (1:1000; Abcam), anti-ubiquitin (1:1000; Protein Tech Group), anti-DNA-PK (1:1000; Santa Cruz Biotechnology, Santa Cruz, CA, USA), anti-DNA-PK pT2609 (1:1000; Rockland, Limerick, PA, USA), anti-β-actin (1:1000; Protein Tech Group), anti-β-tublin (1:1000; Protein Tech Group), or anti-Lamin B (1:1000; Protein Tech Group). After extensive washing with TBST, blots were incubated with IRDye-conjugated secondary antibodies (1:10000; Li-COR Biosciences, Lincoln, NE, USA) for 1 h at room temperature. Immunoreactive bands were imaged using the Odyssey CLx Infrared Imaging system (Li-COR Biosciences).

For co-immunoprecipitation (co-IP), 2 μg of anti-DNA-PK, anti-EGFR or control IgG antibody was incubated with 4 mg of cell lysate, followed by capturing with protein-A/G agarose. The beads were then washed extensively and suspended in SDS loading buffer for western blot analysis.

RT-PCR

RT-PCR was performed with One Step SYBR® PrimeScript™ RT-PCR Kits (Takara Bio, Otsu, Japan) on a Roche 480 Light Cycler (Roche, Basel, Switzerland). The primers used for PCR amplification are shown as follows: 5′-TGTAAGTCAGATGCTCCAACAGG-3′, 5′-TCACCCATTTGTCAAGAACGG-3′ (GOLPH3); 5′-TTTCGATACCCAGGACCAAGCCACAGCAGG-3′ and 5′-AATATT-CTTGCTGGATGCGTTTCTGTA-3′ (EGFR); and 5′-CTGGGACGACATGGAG-

AAAA-3′, 5′-AAGGAAGGCTGGAAGAGTGC-3′ (ACTB). ACTB was used as a normalizing control and data analysis was performed as previously described,[24] through calculating fold change by the $2^{-\Delta\Delta Ct}$ method.

Adenovirus production

To knock down GOLPH3 in xenografts and overexpress EGFR in LUAD cells, the shuttle plasmids, pDC311-U6-GOLPH3-shRNA and pDC315-U6-EGFR, were generated by subcloning human GOLPH3-targeting shRNA oligonucleotides sequences and EGFR cDNA into the shuttle vector pDC311-U6 and pDC315-U6 with ClonExpress® II (Vazyme Biotech Co., Ltd., Nanjing, China), respectively. The shRNA targeting sequences of GOLPH3 were the same as those mentioned above. The adenovirus was then produced by co-transfecting 293A cells with the shuttle plasmids and genomic plasmid (pBHGlox△E1, 3Cre). Adenovirus was harvested, amplified and purified by two rounds of cesium chloride ultracentrifugation. After dialysis, purified adenovirus was aliquoted and stored at -80°C until use. Viral titer was determined by plaque assay.

Xenograft model and treatments

Six-week-old male Balb/c-nude mice were obtained from Model Animal Research Center of Nanjing University (Nanjing, China). All animal studies were conducted according to protocols approved by the Ethical Committee of Experimental Animals of XXXX. Mice were grafted with 1×10^7 A549 cells by subcutaneous injection into the right flank. When tumors reached a size of ~100 mm^3, the tumors were treated with intratumoral injection of 1×10^{10} PFU adenovirus one time per week for two

cycles (two times in total). Two days after each intratumoral injection, tumors were exposed to 6 Gy X-ray with the rest of the body shielded with a lead block. Mice were weighed and tumors were measured every 2 days. The calculation of tumor volume was as follows: $(L\times S^2)/2$ (where L was the longest length and S was the shortest length). The mice were sacrificed 42 d after the first intratumoral injection of adenovirus and all tumors were excised.

Statistical analysis

All experiments were performed at least three times. The data were presented as mean±SD. Differences were calculated by Student's *t* test with SPSS v21.0 software (SPSS, USA), and $p<0.05$ was considered a statistically significant difference.

Results

GOLPH3 over-expresses in human lung adenocarcinoma

To investigate the aberrant expression of GOLPH3 in LUAD, we firstly analyzed the mRNA level of *GOLPH3* in 515 primary tumors and 59 normal tissues based on The Cancer Genome Atlas (TCGA) database by using the online tool UALCAN (http://ualcan.path.uab.edu./analysis.html). As shown in Fig. 1A, significantly elevated *GOLPH3* expression at the mRNA levels was observed in LUAD samples. Further analyses of GOLPH3 protein level with immunohistochemistry in 33 LUAD tissues and 33 adjacent non-tumorous tissues, collected from XXXX, showed a high level of GOLPH3 protein expression (brown staining) in LUAD tissues, whereas low

level in adjacent non-tumorous tissues (Fig. 1B). The quantitative analysis indicated that the MODs of GOLPH3 in LUAD tissues (MOD=0.046±0.027) were significantly higher than those in adjacent non-tumorous tissues (MOD=0.004±0.003) (p<0.001; Fig. 1C). These results indicated that GOLPH3 over-expressed in human LUAD.

Downregulating GOLPH3 sensitizes LUAD cells to IR

Usually, aberrant expression of some genes, especially oncogenes, might cause resistance to radiotherapy. To investigate the role of GOLPH3 in the radioresistance of LUAD, we respectively established stable GOLPH3-knockdown (GOLPH3-KD) A549 and H1299 cell lines. The loss of GOLPH3 protein in GOLPH3-KD cells was confirmed using western blots (Fig. 2A). Survival fractions of GOLPH3-KD A549 and H1299 cells were lower than the respective control (RNAi-NC) after exposure to the same dose of X-ray irradiation (1-6 Gy) (Fig. 2B, C). The sensitization enhancement ratio for D_q ($SERD_q$) in Supplementary Table S1 showed an increase to 1.40 (GOLPH3-RNAi#1) and 2.25 (GOLPH3-RNAi#2) in A549 after GOLPH3 silencing. Similarly, the SERDq of H1299 after GOLPH3 silencing also increased to 1.36 (GOLPH3-RNAi#1) and 1.59 (GOLPH3-RNAi#2) (Fig. 2B, C). Furthermore, the role of GOLPH3 in IR-induced cell death, especially apoptosis, was assessed. The apoptosis rate of GOLPH3-KD cells was significantly higher than RNAi-NC control cells at 72 h after 6 Gy IR (32.43±5.52%, 29.40±2.61% versus 17.10±2.69%) (Fig. 2D, E). The level of cleaved PARP in GOLPH3-KD cells was also higher than that in RNAi-NC control cells after IR (Fig. 2F). Taken together, these results indicated that downregulating GOPLH3 enhanced the sensitivities of A549 and H1299 cells to IR,

and revealed the important role of GOLPH3 in radioresistance in LUAD cells.

GOLPH3 promotes the repair of IR-induced DNA damages

For a further study, MN was assessed after IR as a consequence of accumulated DNA damages. The results in Fig. 3A showed that binucleated MN yields of GOLPH3-KD cells were distinctly higher than those of the RNAi-NC control, which indicated production of more DNA damages or/and lower efficiency of damage repair following GOLPH3 silencing. To analyze the dynamics of DSBs, the most lethal DNA damage after IR, DSBs were assessed by quantifying its marker γ-H2AX. No significant difference in γ-H2AX foci numbers per cell between GOLPH3-KD and RNAi-NC A549 cells was observed at 0.5 h after 4 Gy IR (Fig. 3B, C), which indicated that silencing GOLPH3 did not influence the production of DSBs after IR. However, the γ-H2AX foci numbers per cell in GOLPH3-KD cells were still kept at a high level at 24 h after IR when compared with those of the RNAi-NC control (Fig. 3B, D). The dynamics of DSBs after IR were similar in NC and GOLPH3-KD H1299 cells (Fig. 3E, F), suggesting that silencing GOLPH3 impaired the capacity of DSB repair. Moreover, the capacity of DSB repair was effectively rescued after re-expressing GOLPH3^{Res} in GOLPH3-RNAi#2 cells (Fig. 3G, H), confirming the involvement of GOLPH3 in DSB repair after IR. Residual γ-H2AX protein levels detected at various time-points after IR revealed slower kinetics of DSB repair in GOLPH3-KD cells but almost same after re-expressing GOLPH3 in GOLPH3-KD cells when compared with the RNAi-NC control (Fig. 3I, J), further supporting the key role of GOLPH3 in DSB repair.

GOLPH3 stabilizes epidermal growth factor receptor (EGFR) protein to mediate radioresistance

Both Golgi phosphoprotein 2 (GOLPH2) and GOLPH3 belong to Golgi phosphoprotein family and have some similar functions.[25,26] Ye reported that GOLPH2 is involved in the regulation of EGFR protein level.[27] In addition, we also found that the expression of EGFR was correlated with the GOLPH3 level in various LUAD cell lines (Fig. 4A). Therefore, we hypothesized that GOLPH3 also could regulate EGFR protein in LUAD cells. A direct evidence was that expression of EGFR markedly decreased following GOLPH3 knockdown in A549, H1299 and NCI-H1975 cells (Fig. 4B and Supplementary Fig. 1A). Along with increasing the adenovirus (GOLPH3-RNAi) amount to gradually knockdown GOLPH3, the EGFR protein level showed the same trend with GOLPH3 (Supplementary Fig. 1B). Moreover, EGFR protein level was distinctly restored following the re-expression of $GOLPH3^{Res}$ in GOLPH3-RNAi#2 cells which confirmed the key role of GOLPH3 in regulating the EGFR protein (Fig. 4C). However, no changes in mRNA expression of EGFR, quantified with RT-PCR, were detected in GOLPH3-KD cells (Fig. 4D), which suggested that the loss of EGFR along with GOLPH3 knockdown did not attribute to transcriptional regulation. Considering that the level of EGFR protein was also determined by its stability, we measured the turnover rate of EGFR protein by Cycloheximide (CHX) chase in GOLPH3-KD and control LUAD (A549 and H1299) cells. CHX (100 μg/mL) was used to block total cellular protein synthesis and chase was performed at 4, 8 and 12 h. As shown in Fig. 4E, only small amounts of EGFR

protein, which quickly degraded within 12 h after CHX treatment, were observed in GOLPH3-KD cells. In contrast, EGFR protein was relatively more abundant and highly stable in GOLPH3-NC cells. To investigate how GOLPH3 loss promoted EGFR degradation, we treated cells with MG132 and NH_4Cl to inhibit proteasome and lysosomal activity, respectively. Results showed that NH_4Cl but not MG132 treatment promoted the accumulation of EGFR protein and the accumulation was faster in GOLPH3-KD cells than in GOLPH3-NC cells (Fig. 4F). Since ubiquitination of EGFR was reported to play a key role in the subsequent lysosome-mediated degradation,[28] we next detected the ubiquitylation levels of immunoprecipitated EGFR in GOLPH3-NC and GOLPH3-KD A549 cells. As shown in Fig. 4G, the level of ubiquitinated EGFR in GOLPH3-KD cells was higher than that in GOLPH3-NC cells. These results indicate that loss of GOLPH3 promotes the ubiquitination of EGFR, which is beneficial to the subsequent lysosome-mediated degradation of EGFR. Considering the important role of EGFR in resistance to IR,[29] we hypothesized that radiosensitization mediated by knocking down GOLPH3 benefited from the accompanying and profound decrease of EGFR.

To test this hypothesis, EGFR stable knockdown A549 cells (EGFR-RNAi#1 and EGFR-RNAi#2) were established (Fig. 4H). A lower survival fraction of EGFR-KD cells was observed when compared to that for EGFR-NC cells after the same irradiation dose (Fig. 4H). The $SERD_q$ values were 2.27 and 1.97 for EGFR-RNAi#1 and EGFR-RNAi#2 cells, respectively (Fig. 4H and Supplementary Table S2). These results suggested that loss of EGFR protein significantly increased the radiosensitivity

of A549 cells. To further test whether GOLPH3 mediated radioresistance via regulating EGFR protein, we overexpressed EGFR in GOLPH3-KD A549 cells by adenovirus (Fig. 4I). The survival fraction of GOLPH3-KD cells after IR was increased following EGFR overexpression (Fig. 4J and Supplementary Table S3), providing reliable evidence that GOLPH3 mediated the radioresistance via maintaining the EGFR protein stability.

GOLPH3 facilitates IR-induced nuclear EGFR accumulation and subsequent activation of DNA-PK

It has been reported that EGFR nuclear translocation modulates DNA damage repair following IR treatment, and that inhibiting IR-induced nuclear EGFR accumulation suppressed DNA-PK activity and sensitized cancer cells to IR.[30] Therefore, we wondered whether the level of nuclear EGFR accumulation was impaired following the downregulation of GOLPH3. As shown in Fig. 5A, the immunofluorescence signal of EGFR (red) was dramatically weaker in non-irradiated GOLPH3-KD cells when compared with GOLPH3-NC control. IR (4 Gy) induced the accumulation of EGFR within the nucleus (red/blue) of GOLPH3-NC cells at 20 min and 40 min, but not in GOLPH3-KD cells (Fig. 5A). To further confirm this result, proteins from cell cytoplasm or nucleus were separated. Similar to the results of immunofluorescence, in RNAi-NC cells, the EGFR protein level in the nuclear fraction significantly increased after IR, but no changes were observed in GOLPH3-KD A549 and H1299 cells (Fig. 5B, C). Taken together, these results suggested that decreased IR-induced nuclear EGFR accumulation by silencing

GOLPH3 could be an explanation for the enhancement of radiosensitivity.

Considering that the EGFR is complexed with DNA-PK when transported into the nucleus,[31] co-immunoprecipitation (co-IP) was performed to identify the binding of DNA-PK and EGFR. EGFR co-immunoprecipitated with DNA-PK (Fig. 5D), confirming the physiologic relevance of the interaction. However, the basal and IR-triggered EGFR binding on DNA-PK markedly decreased following GOLPH3 knockdown (Fig. 5D), which was also further confirmed by an immunoprecipitation assay with anti-EGFR antibody (Supplementary Fig. 2). Since activation of DNA-PK linked with IR-induced EGFR nuclear translocation has been reported to be mainly mediated by autophosphorylation at Thr-2609 site,[31,32] activation of DNA-PK was examined in the present work. The results in Fig. 5E, F showed that downregulation of GOLPH3 significantly suppressed IR-induced autophosphorylation of DNA-PK, which meant weaker activation of DNA-PK post-irradiation.

Taken together, knocking down GOLPH3 attenuated the nuclear accumulation of EGFR after IR, which in turn suppressed the activation of DNA-PK, and ultimately inhibited DNA repair to increase the radiosensitivity.

Targeting GOLPH3 enhances IR-induced tumor growth suppress *in vivo*

In vivo studies were performed subsequently. Adenovirus was constructed with high titer (~1.5×10^{11} PFU/mL) to mediate the expression of either empty vector (Ad-RNAi-NC) or GOLPH3 shRNA (Ad-GOLPH3-RNAi#1/ #2) in tumor xenografts. Tumor xenografts were established by subcutaneous injecting A549 cells (~1×10^{7}) into the right flank area of Balb/c-nude mice. When the tumors reached a size ~100

mm^3, the mice were randomly divided into six groups (five mice/ group) as follows: RNAi-NC, RNAi-NC+IR, GOLPH3-RNAi#1, GOLPH3-RNAi#1+IR, GOLPH3-RNAi#2 and GOLPH3-RNAi#2+IR. The treatment of mice was administrated according to the schematic in Fig. 6A. Adenovirus (1×10^{10} PFU/tumor) was injected intratumorally (Day 0) followed by IR (6 Gy) at 48 h after injection with two cycles. The tumor volume was measured every two days. At the end point of measurement (Day 42), the tumor volumes for GOLPH3-RNAi#1+IR and GOLPH3-RNAi#2+IR (305.7±102.8 and 313.0±105.6 mm^3) were significantly smaller than RNAi-NC+IR (586.9±129.3 mm^3) (Fig. 6B, C). The tumor growth curves showed that tumor growth slowed upon IR or GOLPH3 knockdown treatment, but mice treated with IR plus GOLPH3 knockdown showed more significant tumor regression. Moreover, tumors in GOLPH3-RNAi+IR groups nearly stopped growing from Day 12 to Day 32 (Fig. 6C).

The mice were sacrificed on Day 42 and the images of tumors were acquired (Fig. 6D). Results of Ki67 immunohistochemistry revealed a dramatically reduced proliferation index in tumors generated from the treatment with IR plus GOLPH3 knockdown (Fig. 6E). Consistent with the above results, GOLPH3 shRNA treatment enhanced tumor radiosensitivity. The protein level of both GOLPH3 and EGFR in tumors, detected with western blot and immunohistochemistry, showed marked reduction following injection with adenovirus mediated GOLPH3 shRNA expression (Fig. 6F-H). These results suggested that knocking down GOLPH3 effectively enhanced IR-induced tumor xenograft growth suppression.

Discussion

In the present study, we demonstrated that downregulating GOLPH3 expression enhanced the radiosensitivity of LUAD cells both *in vitro* and *in vivo*, and that GOLPH3 played an important role in radioresistance. GOLPH3, characterized as an oncogene, overexpressed in some types of human cancers, including breast cancer,[13] hepatocellular carcinoma,[14] and prostate cancer.[15] Based on RNA-Sequence data (515 lung adenocarcinoma tissues *vs* 59 normal tissues) from TCGA, we found that mRNA of GOLPH3 significantly overexpressed in tumor tissues as compared with normal tissues. Moreover, coincident result with immunohistochemistry was obtained from 33 tumor/normal pairs of LUAD tissues from clinic, and this was also confirmed in previous studies.[17] Importantly, unfavorable clinical outcomes were considered to be associated with overexpression of GOLPH3 in Glioma, hepatocellular carcinoma, breast cancer and NSCLC.[13,14,16,33] However, it has been reported that GOLPH3-positive cancer-associated fibroblasts and tumor-associated macrophages are correlated with the absence of regional or distant metastases of melanoma.[34] Therefore, targeting GOLPH3 needs more comprehensive understanding and needs to be further studied.

In NSCLC patients, GOLPH3 is identified as an oncogene frequently targeted for copy number gain/amplification and high GOLPH3 expression is a potential prognostic biomarker for poor survival.[17,20] Several previous studies have shown overexpression of GOLPH3 confers resistance to DNA-damaging chemotherapeutic drugs, supported by previous results that knocking down GOLPH3 overcame

resistance to doxorubicin and 5-fluorouracil due to increased apoptosis.[19,35] Herein, GOLPH3 associated resistance to radiotherapy, other effective treatment to tumor, was explored. Our results showed that knocking down GOLPH3 impaired DNA damage repair, enhanced cell death and delayed tumor growth after IR. Furthermore, reversal of GOLPH3 depletion rescued the defect in the repair of IR-induced DSBs. Thus, GOLPH3 might be considered as a potential biomarker to evaluate individual radiosensitivity and progression for radiotherapy. Targeting GOLPH3 will be a novel strategy to enhance the radiosensitivity of LUAD. Notably, identification of small molecules to downregulate GOLPH3 expression will be of particular interest towards applications in radiotherapy.

DNA damages especially DSBs inflicted by IR were confirmed as a major factor contributing to IR-induced cell killing.[36] Repair of DSBs exerts powerful influence on radioresistance. An increased capacity for DSB repair confers a survival advantage after IR and shows an enhanced radioresistance.[37] Indeed, DSBs induced by IR can activate complex damage recognition, repair and other cellular response machinery. Various components of the DSBs response, including ATM, ATR, and DNA-PK etc. were also revealed to play important roles in radioresistance, and the corresponding inhibitory small targeting molecules have been developed to serve as potential sensitizers for cancer radiotherapy.[38] Interestingly, Farber-Katz *et al.* reported that the DNA-PK/GOLPH3/MYO18A pathway was required for cell survival following DNA damage.[19] In this pathway, directly phosphorylated GOLPH3 by DNA-PK enhances the interaction of GOLPH3 and MYO18A, and causes Golgi dispersal, impairing

Golgi trafficking to enable cell survival after DNA damage. Unlike Farber-Katz's study, our findings demonstrated that silencing GOLPH3 blocked the phosphorylation of DNA-PK, thereby reducing the DNA-PK kinase activity after irradiation. Undoubtedly, impairment of DNA-PK kinase activity will enhance the radiosensitivity since DNA-PK was one of three major kinases at the "heart" of the DNA damage response.[39] Therefore, a new pathway GOLPH3/EGFR/DNA-PK in response to DSBs after irradiation was revealed in the present work. In addition, our results indicated that interaction between DNA-PK and GOLPH3 might be more complex than initially thought and further studies are warranted to determine the relationship between them.

It is now well appreciated that GOLPH3 is a highly conserved protein enriched at the trans-Golgi network (TGN),[20] whereas DNA damage repair mainly takes place in the nucleus. Whether GOLPH3 translocated into nucleus to participate in the DSB repair is still unclear. However, we did not observe the recruitment of GOLPH3 protein to the DSB sites and even translocation into nucleus after irradiation (Supplementary Fig. 3A, B). Thus a mediator could be required to link GOLPH3 to DSB repair. In fact, our data suggested that EGFR played a crucial role in DSB repair as a link between GOLPH3 and DNA-PK. Previous studies have confirmed that IR initiates internalization and nuclear translocation of EGFR by phosphorylating its residue Thr654 and Tyr845 and then increases the activity of DNA-PK.[32,40] In our study, a positive correlation has been found between EGFR and GOLPH3 proteins in various LUAD cell lines and knocking down GOLPH3 reduces the raidoresistance of

LUAD cells *via* decreasing nuclear EGFR protein level and DNA-PK activity, suggesting the key role of GOLPH3/EGFR/DNA-PKcs signal axis in radioresistance of LUAD cells. Undoubtedly, EGFR mutations may affect the role of GOLPH3/EGFR/DNA-PKcs signal axis in radioresistance since EGFR with activating mutations, L858R or ΔE746-E750, are defective in radiation-induced translocation into the nucleus and fail to activate the DNA-PK.[41,42] Therefore, the effect of GOLPH3 on the radioresistance of LUAD cells with mutant EGFR needs to be further studied. Moreover, it has been reported that the activation of EGFR after radiation is affected by cell cycle, and EGFR inhibitors may reduce the radiosensitivity in quiescent tumor cells but enhance the radiosensitivity in proliferating cells.[43] Considering that GOLPH3 regulates EGFR protein levels, whether the effect of GOLPH3 on radiosensitivity is affected by cell cycle is also still a question that needs further studies in the future.

Recent studies report that some members of Golgi phosphoprotein family are involved in the regulation of EGFR stability. GOLPH2 (also named GOLM1) complexed with Rab11 and EGFR assist the recycling of EGFR back to plasma membrane instead of following the degradation pathway, thereby preventing EGFR degradation.[27] Scott *et al.* have reported that GOLPH3 transports to the endosomal and the plasma, and regulates receptor recycling of key molecules.[44] It is noted that GOLPH3 depletion expedites the internalization of EGFR after EGF stimulation and promotes EGFR endocytosis and degradation *via* activating Rab5.[33] Although our results indicated that knocking down GOLPH3 was able to promote the ubiquitination

and degradation of EGFR without extra EGF stimulation, fetal bovine serum (FBS) in cell culture medium also contains EGF. It was possible that GOLPH3 modulated the stability of EGFR by sharing the same molecular mechanisms. Indeed, further studies would be needed to confirm this conjecture. In addition, we also observed that loss of GOLPH3 also reduced the level of other receptor tyrosine kinases (RTKs) such as PDGFR and VEGFR2 (Supplementary Fig. 4A, B), which take part in proliferation, migration and invasion of tumor cells.[45,46] As such, targeting GOLPH3 might have multiple effects in reducing cancer risk and progression by decreasing multiple RTKs.

Our results demonstrated that GOLPH3 promoted DSB repair after irradiation by sustaining stability of EGFR, which is necessary for DNA-PK activation. Our findings provided a strong support to that the expression level of GOLPH3 in LUAD was tightly associated with the radioresistance and targeting GOLPH3 might be a therapeutic strategy for sensitization in LUAD radiotherapy.

References

1. Sung H, Ferlay J, Siegel RL, et al. Global cancer statistics 2020: Globocan estimates of incidence and mortality worldwide for 36 cancers in 185 countries. *CA Cancer J Clin* 2021;71:209-249.
2. Siegelin MD, Borczuk AC. Epidermal growth factor receptor mutations in lung adenocarcinoma. *Lab Invest* 2014;94:129-137.
3. Johung KL, Yao X, Li F, et al. A clinical model for identifying radiosensitive tumor genotypes in non-small cell lung cancer. *Clin Cancer Res* 2013;19:5523-5532.
4. Xie J, Li Y, Jiang K, et al. Cdk16 phosphorylates and degrades p53 to promote radioresistance and predicts prognosis in lung cancer. *Theranostics* 2018;8:650-662.
5. Lu L, Dong J, Wang L, et al. Activation of stat3 and bcl-2 and reduction of reactive oxygen species (ros) promote radioresistance in breast cancer and overcome of radioresistance with niclosamide. *Oncogene* 2018;37:5292-5304.
6. Chakravarti A, Dicker A, Mehta M. The contribution of epidermal growth factor receptor (egfr) signaling pathway to radioresistance in human gliomas: A review of preclinical and correlative clinical data. *Int J Radiat Oncol Biol Phys* 2004;58:927-931.
7. Brand TM, Iida M, Luthar N, et al. Nuclear egfr as a molecular target in cancer. *Radiother Oncol* 2013;108:370-377.
8. Bethune G, Bethune D, Ridgway N, et al. Epidermal growth factor receptor

(egfr) in lung cancer: An overview and update. *J Thorac Dis* 2010;2:48-51.

9. Pirker R, Pereira JR, Von Pawel J, et al. Egfr expression as a predictor of survival for first-line chemotherapy plus cetuximab in patients with advanced non-small-cell lung cancer: Analysis of data from the phase 3 flex study. *Lancet Oncol* 2012;13:33-42.

10. Das AK, Chen BP, Story MD, et al. Somatic mutations in the tyrosine kinase domain of epidermal growth factor receptor (egfr) abrogate egfr-mediated radioprotection in non-small cell lung carcinoma. *Cancer Res* 2007;67:5267-5274.

11. Milas L, Fan Z, Andratschke NH, et al. Epidermal growth factor receptor and tumor response to radiation: In vivo preclinical studies. *Int J Radiat Oncol Biol Phys* 2004;58:966-971.

12. Liccardi G, Hartley JA, Hochhauser D. Egfr nuclear translocation modulates DNA repair following cisplatin and ionizing radiation treatment. *Cancer Res* 2011;71:1103-1114.

13. Zeng Z, Lin H, Zhao X, et al. Overexpression of golph3 promotes proliferation and tumorigenicity in breast cancer via suppression of the foxo1 transcription factor. *Clin Cancer Res* 2012;18:4059-4069.

14. Dai T, Zhang D, Cai M, et al. Golgi phosphoprotein 3 (golph3) promotes hepatocellular carcinoma cell aggressiveness by activating the nf-κ b pathway. *J Pathol* 2015;235:490-501.

15. Hua X, Yu L, Pan W, et al. Increased expression of golgi phosphoprotein-3 is

associated with tumor aggressiveness and poor prognosis of prostate cancer. *Diagn Pathol* 2012;7:127.

16. Zhang Y, Ma M, Han B. Golph3 high expression predicts poor prognosis in patients with resected non-small cell lung cancer: An immunohistochemical analysis. *Tumor Biol* 2014;35:10833-10839.
17. Tang W, Han M, Ruan B, et al. Overexpression of golph3 is associated with poor survival in non-small-cell lung cancer. *Am J Transl Res* 2016;8:1756-1762.
18. Zhang Q, Zhuang J, Deng Y, et al. Mir34a/golph3 axis abrogates urothelial bladder cancer chemoresistance via reduced cancer stemness. *Theranostics* 2017;7:4777-4790.
19. Farber-Katz SE, Dippold HC, Buschman MD, et al. DNA damage triggers golgi dispersal via DNA-pk and golph3. *Cell* 2014;156:413-427.
20. Scott KL, Kabbarah O, Liang M-C, et al. Golph3 modulates mtor signalling and rapamycin sensitivity in cancer. *Nature* 2009;459:1085-1090.
21. Zhu S, Wang H, Ding S. Reprogramming fibroblasts toward cardiomyocytes, neural stem cells and hepatocytes by cell activation and signaling-directed lineage conversion. *Nat Protoc* 2015;10:959-973.
22. Franken NA, Rodermond HM, Stap J, et al. Clonogenic assay of cells in vitro. *Nat Protoc* 2006;1:2315-2319.
23. Fenech M. Cytokinesis-block micronucleus cytome assay. *Nat Protoc* 2007;2:1084-1104.
24. Livak KJ, Schmittgen TD. Analysis of relative gene expression data using

real-time quantitative pcr and the 2− ΔΔct method. *Methods* 2001;25:402-408.

25. Kim H-J, Lv D, Zhang Y, et al. Golgi phosphoprotein 2 in physiology and in diseases. *Cell Biosci* 2012;2:31.

26. Sechi S, Frappaolo A, Belloni G, et al. The multiple cellular functions of the oncoprotein golgi phosphoprotein 3. *Oncotarget* 2015;6:3493-3506.

27. Ye Q-H, Zhu W-W, Zhang J-B, et al. Golm1 modulates egfr/rtk cell-surface recycling to drive hepatocellular carcinoma metastasis. *Cancer Cell* 2016;30:444-458.

28. Eden ER, Huang F, Sorkin A, et al. The role of egf receptor ubiquitination in regulating its intracellular traffic. *Traffic* 2012;13:329-337.

29. Petrás M, Lajtos T, Friedländer E, et al. Molecular interactions of erbb1 (egfr) and integrin-β1 in astrocytoma frozen sections predict clinical outcome and correlate with akt-mediated in vitro radioresistance. *Neuro Oncol* 2013;15:1027-1040.

30. Han W, Lo H-W. Landscape of egfr signaling network in human cancers: Biology and therapeutic response in relation to receptor subcellular locations. *Cancer Lett* 2012;318:124-134.

31. Dittmann K, Mayer C, Fehrenbacher B, et al. Radiation-induced epidermal growth factor receptor nuclear import is linked to activation of DNA-dependent protein kinase. *J Biol Chem* 2005;280:31182-31189.

32. Dittmann K, Mayer C, Kehlbach R, et al. Radiation-induced caveolin-1 associated egfr internalization is linked with nuclear egfr transport and

activation of DNA-pk. *Mol Cancer* 2008;7:69.

33. Zhou X, Xie S, Wu S, et al. Golgi phosphoprotein 3 promotes glioma progression via inhibiting rab5-mediated endocytosis and degradation of epidermal growth factor receptor. *Neuro Oncol* 2017;19:1628-1639.

34. Donizy P, Kaczorowski M, Biecek P, et al. Golgi-related proteins golph2 (gp73/golm1) and golph3 (gopp1/midas) in cutaneous melanoma: Patterns of expression and prognostic significance. *Int J Mol Sci* 2016;17.

35. Wang Z, Jiang B, Chen L, et al. Golph3 predicts survival of colorectal cancer patients treated with 5-fluorouracil-based adjuvant chemotherapy. *J Transl Med* 2014;12:15.

36. Santivasi WL, Xia F. Ionizing radiation-induced DNA damage, response, and repair. *Antioxid Redox Sign* 2014;21:251-259.

37. Desai A, Webb B, Gerson SL. Cd133+ cells contribute to radioresistance via altered regulation of DNA repair genes in human lung cancer cells. *Radiother Oncol* 2014;110:538-545.

38. O'connor M, Martin N, Smith G. Targeted cancer therapies based on the inhibition of DNA strand break repair. *Oncogene* 2007;26:7816-7824.

39. Blackford AN, Jackson SP. Atm, atr, and DNA-pk: The trinity at the heart of the DNA damage response. *Mol Cell* 2017;66:801-817.

40. Dittmann K, Mayer C, Fehrenbacher B, et al. Nuclear egfr shuttling induced by ionizing radiation is regulated by phosphorylation at residue thr654. *FEBS Lett* 2010;584:3878-3884.

41. Das AK, Sato M, Story MD, et al. Non-small-cell lung cancers with kinase domain mutations in the epidermal growth factor receptor are sensitive to ionizing radiation. *Cancer Res* 2006;66:9601-9608.

42. Das AK, Chen BP, Story MD, et al. Somatic mutations in the tyrosine kinase domain of epidermal growth factor receptor (egfr) abrogate egfr-mediated radioprotection in non-small cell lung carcinoma. *Cancer Res* 2007;67:5267-5274.

43. Ahsan A, Hiniker SM, Davis MA, et al. Role of cell cycle in epidermal growth factor receptor inhibitor-mediated radiosensitization. *Cancer Res* 2009;69:5108-5114.

44. Scott KL, Chin L. Signaling from the golgi: Mechanisms and models for golgi phosphoprotein 3-mediated oncogenesis. *Clin Cancer Res* 2010;16:2229-2234.

45. Cao Y. Multifarious functions of pdgfs and pdgfrs in tumor growth and metastasis. *Trends Mol Med* 2013;19:460-473.

46. Silva SR, Bowen KA, Rychahou PG, et al. Vegfr-2 expression in carcinoid cancer cells and its role in tumor growth and metastasis. *Int J Cancer* 2011;128:1045-1056.

Figure Captions

Fig. 1. GOLPH3 over-expressed in LUAD clinical tissue samples. (A) GOLPH3 mRNA levels in normal and LUAD tissues (based on TCGA database). (B) Representative images of GOLPH3 immunohistochemistry in adjacent nontumorous and LUAD tissues. Scale bar: 40 μm. (C) Statistical quantification of the average MOD of GOLPH3 staining in adjacent nontumorous (n=33) and LUAD (n=33) tissues.

Fig. 2. Loss of GOLPH3 sensitizing LUAD cells to IR. (A) Determination of GOLPH3 knockdown in A549 and H1299 cells. (B) Representative images of the colonies from RNAi-NC and GOLPH3-RNAi A549 and H1299 cells after IR. (C) The survival curves of RNAi-NC and GOLPH3-RNAi A549 and H1299 cells after IR. (D) Representative results of flow cytometry depicting apoptosis of RNAi-NC and GOLPH3-RNAi H1299 cells at 72 h after IR (6 Gy). (E) Quantification of apoptosis ratio in RNAi-NC and GOLPH3-RNAi H1299 cells. (★: $p<0.05$). (F) Western blot of cleaved PARP in RNAi-NC and GOLPH3-RNAi H1299 cells at 72 h after IR (6 Gy). The number below each band represents the relative level of cleaved PARP/ PARP.

Fig. 3. GOLPH3 participating in the repair of IR-induced DSBs. (A) MN yields in RNAi-NC and GOLPH3-RNAi cells after IR. (★: $p<0.05$). (B) Representative immunofluorescence images of γ-H2AX foci (red) in nucleus (blue) of RNAi-NC and GOLPH3-RNAi A549 cells at 0.5 and 24 h after IR (4 Gy). Scale bar: 20 μm. (C)

Quantifying γ-H2AX foci at 0.5 h to evaluate DSBs production after IR (4 Gy) in RNAi-NC and GOLPH3-RNAi A549 cells. (D) Quantifying of γ-H2AX foci at 24 h after IR to evaluate the residual DSBs in RNAi-NC and GOLPH3-RNAi A549 cells. (★: $p<0.05$; ★ ★ : $p<0.01$). (E) Representative immunofluorescence images of γ-H2AX foci (red) in nucleus (blue) of RNAi-NC and GOLPH3-RNAi H1299 cells at 0.5 and 24 h after IR (4 Gy). Scale bar: 20 μm. Quantitative data are depicted in (F). (G) Representative immunofluorescence images of γ-H2AX foci at 0.5 and 24 h post IR (4 Gy) following GOLPH3 re-expression in GOLPH3-KD A549 cells. Scale bar: 10 μm. Quantitative data are depicted in (H)**.** (I) Western blot of γ-H2AX protein level at multiple time points after IR (4 Gy). The number below each band represents the relative expression level of γ-H2AX. (J) Western blot of γ-H2AX protein level at multiple time points after IR (4 Gy) following GOLPH3 re-expression in GOLPH3-KD A549 cells. The number below each band represents the relative expression level of γ-H2AX.

Fig. 4. GOLPH3 confers radioresistance by regulating the stability of EGFR. (A) Western blot of GOLPH3 and EGFR expression in seven LUAD cell lines. (B) Western blot of EGFR protein expression in RNAi-NC/GOLPH3-RNAi A549 and H1299 cells. (C) Western blot of EGFR, GOLPH3 and $GOLPH3^{Res}$ protein expression following the re-expression of GOLPH3 in GOLPH3-RNAi#2 A549 and H1299 cells. The number below each band represents the relative expression level of EGFR. (D) Quantitative PCR detection of the relative expression of GOLPH3 and EGFR

transcripts in RNAi-NC/GOLPH3-RNAi A549 and H1299 cells. (E) RNAi-NC/GOLPH3-RNAi A549 and H1299 cells were treated with CHX (100 μg/mL) for indicated time. Then cells were lysed and EGFR protein expression analyzed by western blot. The number below each band represents the relative expression level of EGFR. (F) RNAi-NC/GOLPH3-RNAi A549 and H1299 cells were treated with MG132 (20 μM) or NH_4Cl (20 mM) for 48 h. Then cells were lysed and EGFR protein expression analyzed by western blot. The number below each band represents the relative expression level of EGFR. (G) Western blot detection of the ubiquitination levels of EGFR immunoprecipitated from RNAi-NC and GOLPH3-RNAi A549 cells. (H) The survival curves of RNAi-NC and EGFR-RNAi A549 cells after IR. (I) Western blot of EGFR protein level in indicated cells after EGFR overexpression mediated by adenovirus. The number below each band represents the relative expression level of EGFR. (J) The survival curves of RNAi-NC and EGFR-RNAi A549 cells following EGFR overexpression after IR.

Fig. 5. GOLPH3 knockdown impairs the IR-induced EGFR nuclear import and activation of DNA-PK. (A) Representative immunofluorescence images of EGFR (red) in RNAi-NC and GOLPH3-RNAi A549 cells at 20 and 40 min post IR (4 Gy). Nucleus (blue) was stained with DAPI. Scale bar: 10 μm. Western blot of EGFR in the cytoplasmic and nuclear fractions of RNAi-NC/GOLPH3-RNAi (B) A549 and (C) H1299 cells treated with IR (4 Gy). The cytoplasmic and nuclear proteins were separated at 20 and 40 min after IR. β-Tublin and Lamin B used as loading controls of

cytoplasmic and nuclear proteins respectively. The number below each band represents the relative expression level of EGFR. (D) Western blot of anti-DNA-PK immunoprecipitates from RNAi-NC and GOLPH3-RNAi A549 cells after IR (4 Gy). The number below each band represents the relative level of EGFR/DNA-PK. (E) Western blot of DNA-PK phosphorylation induced by IR (4 Gy) in RNAi-NC and GOLPH3-RNAi A549 cells. Quantitative data are depicted in (F) *, $p<0.05$.

Fig. 6. Silencing of GOLPH3 expression increases radiation-induced tumor xenograft growth delay *in vivo*. (A) Schematic showing the treatment for Balb/c-nude mice bearing A549 xenograft. Adenovirus was intratumorally injected at day 0 and day 7 respectively. Tumors were irradiated with 6 Gy X-ray at 48 hours after each adenovirus injection. (B) Images of nude mice bearing tumors at day 42. (C) Tumor volume. From day 0, tumors were measured every two days. Tumor volumes were calculated and data were plotted using the geometric mean for each group vs. time. Each point represents the mean tumor volume (Mean±SD) of measurements from each group (n=5). (D) Images of tumors acquired from nude mice at day 42. (E) Representative immunohistochemistry images and quantification of Ki67 in RNAi-NC and GOLPH3-RNAi tumor. Scale bar: 50 μm. (F) Western blot of EGFR and GOLPH3 in tumor tissues from each group. The number below each band represents the relative expression level of EGFR or GOLPH3. (G) Representative immunohistochemistry images and quantification of GOLPH3 in RNAi-NC and GOLPH3-RNAi tumor. Scale bar: 50 μm. (H) Representative immunohistochemistry

images and quantification of EGFR in RNAi-NC and GOLPH3-RNAi tumor. Scale bar: 50 μm.

Fig. 1

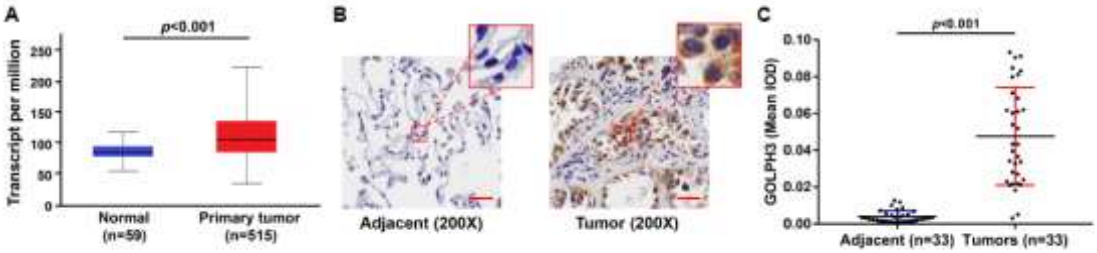

Fig. 2

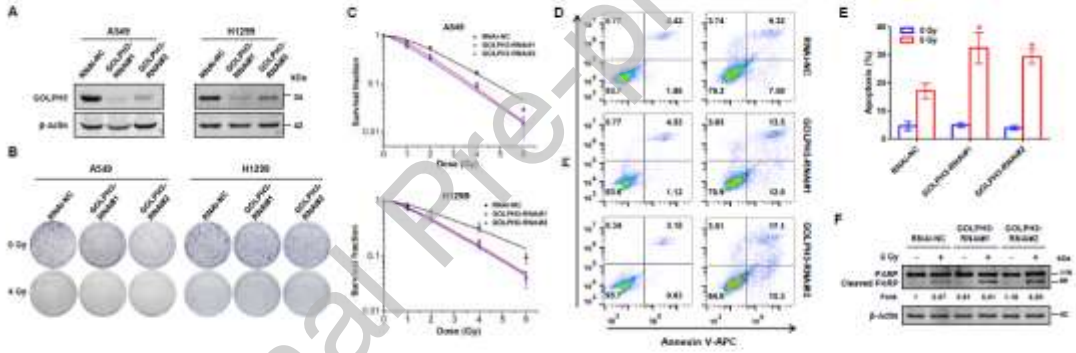

Fig. 3

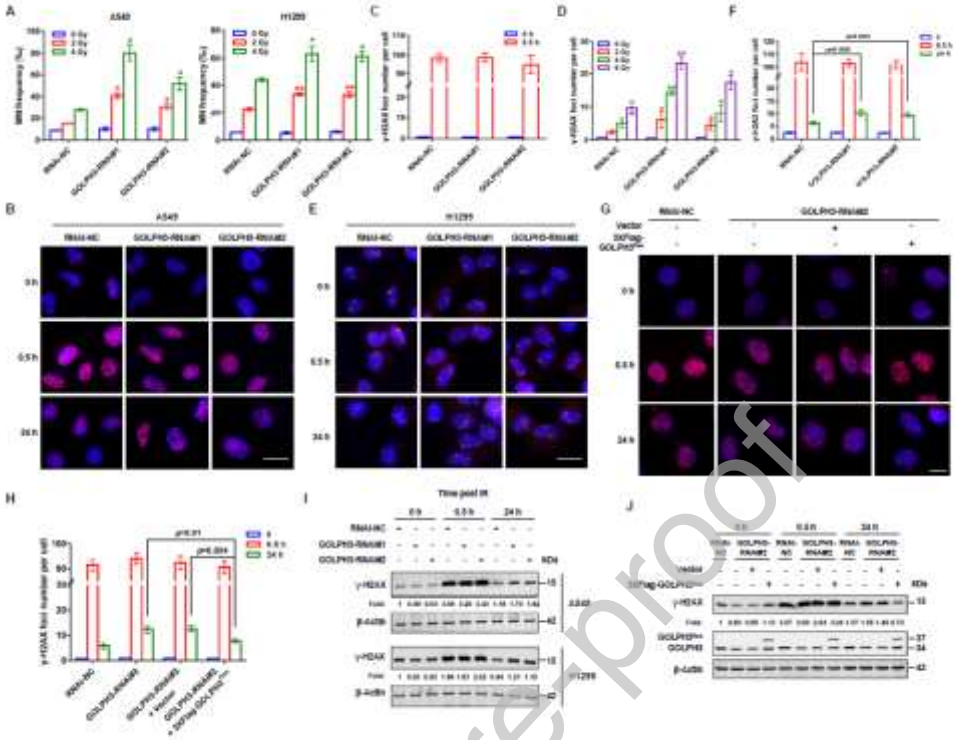

Fig. 4

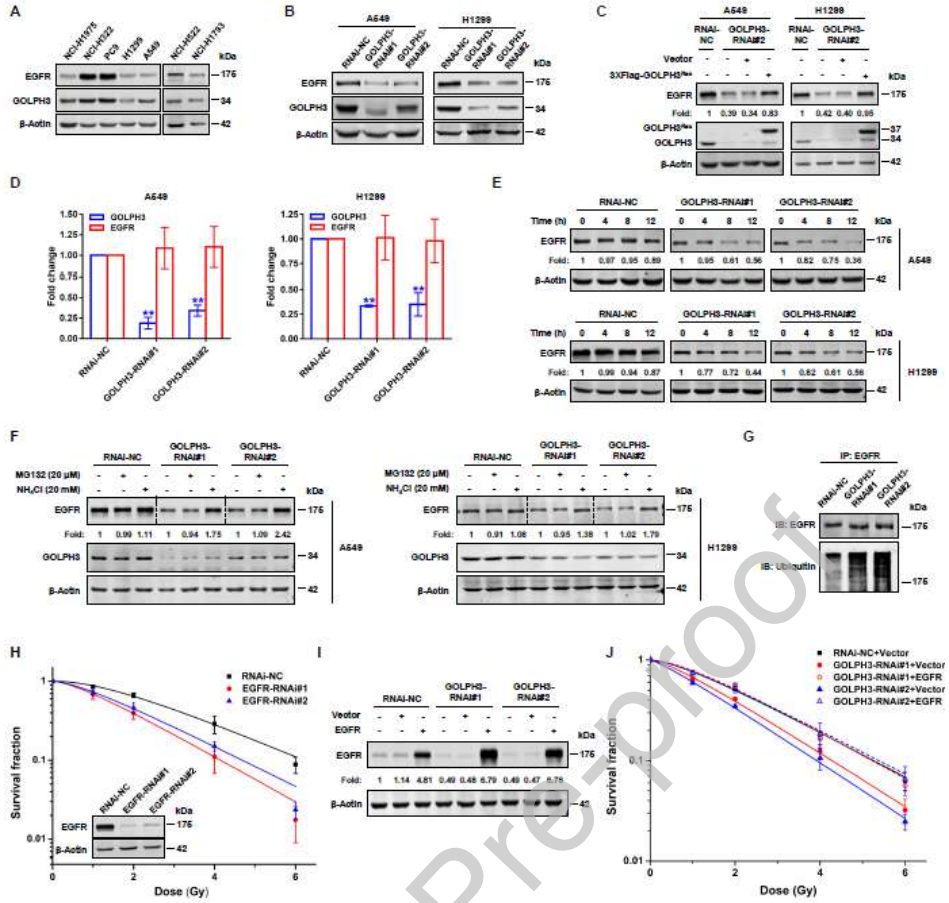

Fig. 5

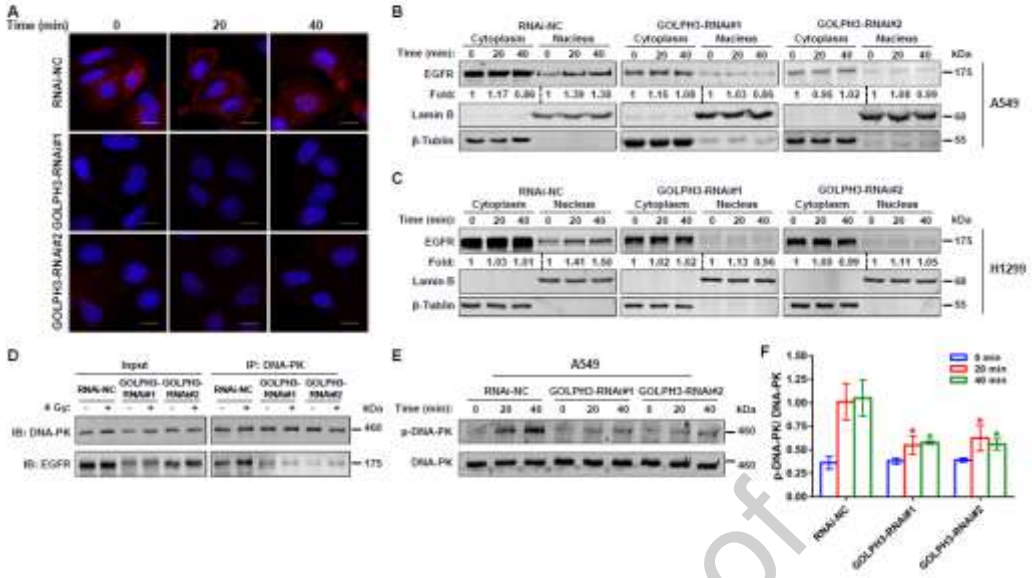

Fig. 6